

Ferroelectric effect in oxide based pyro-phototronic photodetector

Abstract. Growing number of photodetectors in use might require sheer amounts of energy to power them and in order to prevent that, studies on self-powered detectors are gaining more popularity. A common approach synergistically couples multiple effects, to combine all of their advantages. In this work we attempt to refine characteristics of a pyro-phototronic device, based on Si/SnO_x/ZnO heterojunction, by the introduction of a ferroelectric BCZT (0.5Ba(Zr_{0.2}Ti_{0.8})O₃–0.5(Ba_{0.7}Ca_{0.3})TiO₃) layer. The influence of the ferroelectric polarization on the performance of the detector is observed, however the enhancement of electric field does not result in improvement of detection parameters.

Streszczenie. Rosnąca liczba fotodetektorów używanych dookoła nas może w przyszłości wymagać ogromnych nakładów energii do zasilania. By temu zapobiec, popularnym przedmiotem badań są fotodetektory samozasilające, powszechnie opierające się na strukturach wykorzystujących jednocześnie wiele różnych efektów. W tej pracy staramy się poprawić parametry detektora pirofototronicznego bazującego na złączu Si/SnO_x/ZnO, wprowadzając do niego ferroelektryczną warstwę BCZT (0.5Ba(Zr_{0.2}Ti_{0.8})O₃–0.5(Ba_{0.7}Ca_{0.3})TiO₃). Obserwujemy wpływ polaryzacji ferroelektryka na osiągnięci urządzenia, jednak zwiększenie pola elektrycznego nie skutkuje poprawą parametrów detekcji. (Zjawisko ferroelektryczne w fotodetektorze bazującym na tlenkach wykorzystującym efekt pirofototroniczny).

Keywords: ferroelectricity, self-powered photodetector, polarization-controlled response, carrier separation

Słowa kluczowe: ferroelektryczność, samo-zasilający się fotodetektor, odpowiedź modulowana polaryzacją, separacja nośników

Introduction

Photodetectors are basic electronic devices whose applications range from telecommunications, through environment monitoring to medicine [1]. Conventional implementations of such devices require external biasing voltage to achieve good photodetection parameters. In the era of IoT (“Internet of Things”), photodetectors find new use cases every day, it is thus important, both from environmental and applicational perspectives, to reduce their power consumption.

Among many attempts to design a self-powered detector, a hybrid approach, harnessing both photovoltaic and pyroelectric effects, was proposed by Wang in 2015 [2]. Pyroelectric effect generates spontaneous polarization across the layer due to a temperature gradient originating from light absorption in the material. Electric field connected with induced polarization enhances the built in potential in a semiconductor junction of a photovoltaic device, improving separation of electron-hole pairs generated by absorption of a photon, thus increasing resulting current output and improving photodetection properties such as responsivity, sensitivity, detectivity, rise- and fall-times. [3] Similar improvement can be achieved by introducing other sources of electric field such as piezoelectric effect [4], [5] or ferroelectric effect [6]. Utilizing the latter one, detection parameters can be easily modulated with polarization determined by poling voltage [7].

Great part of ferroelectric ceramics contain lead, which due to its toxicity disqualifies them from broad application. In recent years, the lead free alternatives gain more attention for this very reason. One of those alternatives, 0.5Ba(Zr_{0.2}Ti_{0.8})O₃–0.5(Ba_{0.7}Ca_{0.3})TiO₃ (BCZT), is characterized by a high value of piezoelectric coefficient of d₃₃ ~620 pC/N [8] while also having high pyroelectric coefficient of 5.0 × 10⁻⁴ C/m²K [9] when compared to others (e.g. Bi_{0.5}Na_{0.5}TiO₃ – 50 nC/m²K or BaTiO₃ – 16 nC/m²K [10], [11]).

We chose to introduce BCZT to a SnO and ZnO based pyro-phototronic device, which we have presented in 2021 [12]. The device coupled good photovoltaic properties of n-Si/p-SnO_x junction (power conversion efficiency (PCE) of

8.3% [13]) with pyroelectric ZnO 1.5 nC/m²K [11] resulting with superb photodetection properties of responsivity R=64 mA/W, detectivity D* = 2.4 × 10¹¹ Jones and response time τ_r = 2 μs. Electric field resulting from ferroelectric material is expected to enhance the carrier separation at the p-n junction

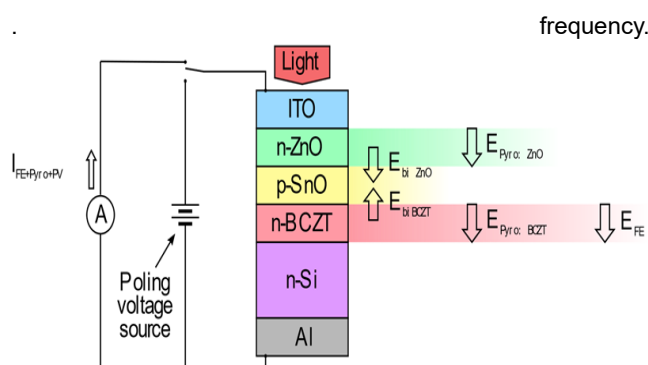
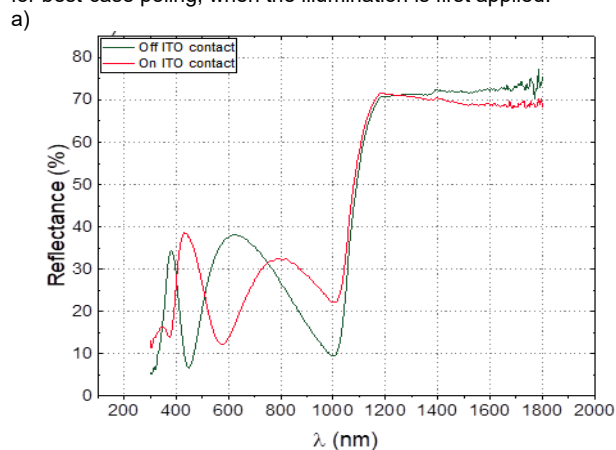


Fig 1. Al/n-Si/n-BCZT/p-SnO_x/n-ZnO/ITO device structure (center), electrical connections (left), electric fields present in different layers for best-case poling, when the illumination is first applied.



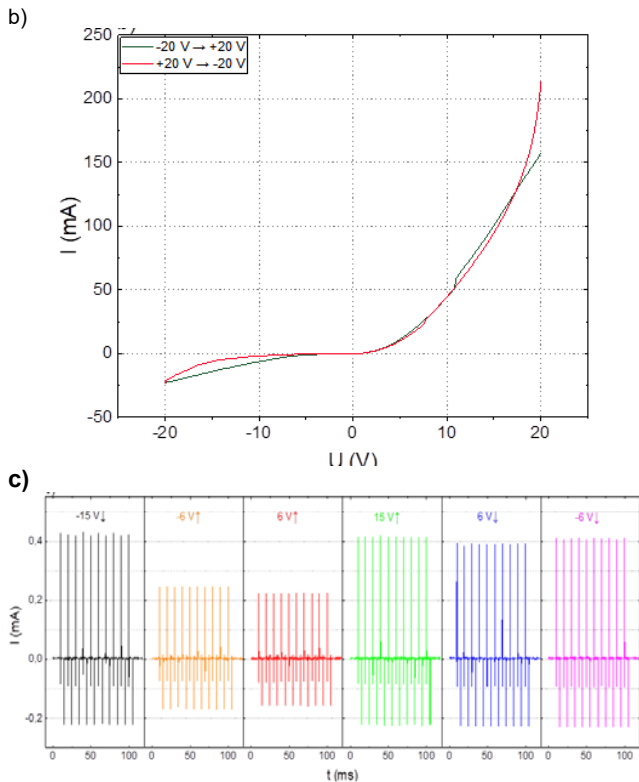


Fig. 2. a) Reflectance spectra of the Al/n-Si/n-BCZT/p-SnO_x/n-ZnO/ITO device; b) I-V characteristics measured in both directions; c) total current recorded (I-t curves) for different poling voltages under 650 nm laser illumination with power density of 10.9 mW/cm² and 100 Hz chopping frequency

Experimental methods

The device investigated in this work was produced as a Al/n-Si/n-BCZT/p-SnO_x/n-ZnO/ITO structure, depicted on figure 1. On the silicon substrate thin films of tin-oxide, zinc-oxide and transparent electrode (ITO) were grown as described previously in [12], while BCZT layer was deposited as reported in [14]. Aluminum back electrode was attached to the substrate by electric spark.

Optical properties (reflectance) of the device were measured using Bentham PVE300 setup. Current-time (I-t) characteristics were captured using a self-built setup, consisting of a Keithley 428 current amplifier and a National Instruments PCI-6251 I/O card, controlled by LabVIEW based software. The sample was illuminated by a 445 nm and 650 nm semiconductor lasers, electronically modulated with 50% duty cycle PWM signal generated by the I/O card. Repetition rates of 10, 20, 50, 100, 200 and 400 Hz were applied during measurements. Poling was performed by applying a 10 s voltage pulse ranging from -15 to 15 V with a help of a Keithley 2601A source-meter. Finally, the same device was used for Current-Voltage (I-V) characteristics. All measurements were performed in normal conditions.

Results and discussion

Figure 2a) shows reflectance spectra of the Si/BCZT/SnO/ZnO structure, measured both on- and off-the ITO contact. The fringes in the low-wavelength parts indicate that interference occurs, confirming thin-film structure of the sample. Moving to lower energies, a rapid reflectance increase, connected with absorption edge of the Si substrate, can be observed. A laser wavelength of 650 nm was chosen for further measurements, due to its proximity to the reflectance valley, in order to maximize the number of photons reaching the absorber.

I-V characteristics, visible in figure 2b), were measured in range of -20 to 20 V in both directions. Their asymmetry indicates that the structure can be treated as a diode. Different behavior of the up and down curves can be explained by the presence of the ferroelectric layer. Depending on the poling, the electric field inside this layer is changing the direction, in one case the same as the build in field in p-n junction, in the other the reverse.

Transient response of characteristics were first investigated under zero bias and zero poling with previously selected 650 nm laser illumination as a function of laser power and chopping frequency. The typical pyro-phototronic response, as observed in figure 2c), was present for all applied frequencies and power densities. Averaged values of pyro-phototronic current (over 100 light pulses in fixed conditions), visible in figure 3a), show minor influence of frequency on the output of the detector and current saturation in high illumination power region.

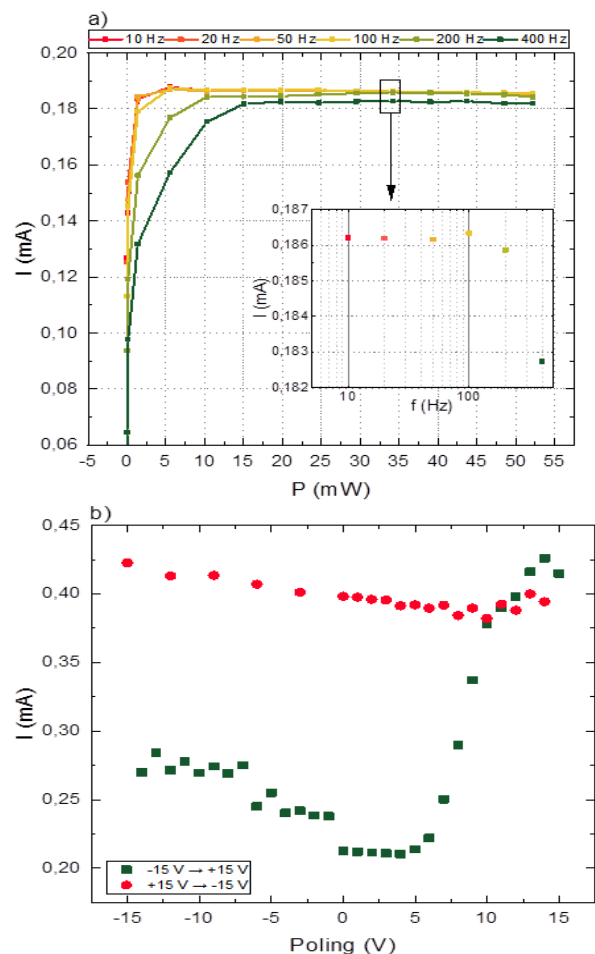


Fig 3. a) Total current generated by the device under fixed 650 nm laser illumination without poling as a function of laser power and chopping frequency; b) total current generated by the device under fixed 650 nm laser illumination with power density of 10.9 mW/cm² and 100 Hz chopping frequency as a function of poling voltage.

The saturation can be assigned to the sample heating up as a whole structure, changing heat distribution in the sample while also affecting heat dissipation to surrounding air. This in turn effectively reduces the temperature gradient which is responsible for pyroelectric effect.

To investigate the ferro-pyro-phototronic effect in the structure, laser power and chopping frequency were fixed at 10.9 mW/cm² and 100 Hz, then poling voltage in range of -20 to 20 V was applied. I-t curves for few different voltages are shown in figure 2c). Poling voltage has a noticeable

impact on the current maxima and changes of those values follow a loop presented in figure 3b). Such behavior does fit our expectations and can be explained as following with the help of electric fields illustrated on figure 1.

When the illumination is first applied, electron-hole pairs are generated in silicon absorber and due to proximity to the semiconductor junction, are separated by built-in electric field E_{bi} . The separation of the carriers is not fully efficient which causes some of the absorbed energy to be converted to heat, producing a temperature gradient responsible for pyroelectric polarization E_{pyro} . The ferroelectric layer, which we introduced to the device in this research, retains the electric field applied during poling. All of the fields E_{bi} , E_{pyro} and E_{FE} add together and are responsible for separation of the carriers. When opposite poling is applied, the direction of E_{FE} is reversed, which results in diminution of the total electric field. When the illumination is turned off, the sample begins to cool down, which generates opposite pyroelectric polarization and induces negative current.

Responsivity (R), detectivity (D^*) and sensitivity (S), given by equations 1,2 and 3 respectively (where I_{Light} and I_{Dark} – short-circuit current and without illumination; P and A – effective illumination power and area; q – elementary charge) also behave in a loop like fashion. Results for best poling conditions are shown in Table 1.

$$(1) \quad R = \frac{I_{Light} - I_{Dark}}{P}$$

$$(2) \quad D^* = R \left(\frac{A}{2 \cdot q \cdot I_{Dark}} \right)^{1/2}$$

$$(3) \quad S = \frac{I_{Light} - I_{Dark}}{I_{Dark}}$$

Table 1. Summary of the results and comparison with other works.

Photodetector	λ (nm)	R (mA/W)	D^* (Jones)	S	Ref.
Al/Si/BCZT/SnO _x /ZnO/ITO	650	12	1.0×10 ⁹	1.5×10 ⁵	This work
Al/Si/SnO _x /ZnO/ITO	405	37	1.5×10 ¹¹		[12]
	650	64	2.4×10 ¹¹		
Al/Si/SiO _x /BCZT/ITO	405	13	1.7×10 ¹⁰		[7]
Ag/Si/ZnO NWs/ITO	670	~0.16	~4×10 ¹⁰		[15]
Pyramid					
Al/p-Si/n-ZnO NWs/ITO	648	0.76			[16]

Conclusion

A Si/BCZT/SnO_x/ZnO heterostructure was proposed as a possible refinement of an excellent pyro-phototronic detector by introduction of the ferroelectric BCZT layer. We have shown the influence of the poling voltage on the performance of the detector, indicating that the ferroelectric effect does play a significant role in the carrier transport in the device. Detection parameters – especially responsivity – while being competitive with other structures, turned out to be worse than those reported for the reference structure without the BCZT layer. The deterioration can be partially attributed to a negligible contribution of photocurrent generated in the n-BCZT/p-SnO_x junction. Overall, results suggest that for further enhancement of detection parameters, the quality of a semiconductor junction is equally important as the electric field present in the junction.

Acknowledgments

The research was partially supported by the statutory grant (No. 8211104160) of Department of Quantum Technologies of Wrocław University of Science and Technology.

REFERENCES

- [1] Y. Wang, L. Zhu, Y. Feng, Z. Wang, and Z. L. Wang, "Comprehensive Pyro-Phototronic Effect Enhanced Ultraviolet Detector with ZnO/Ag Schottky Junction," *Adv. Funct. Mater.*, vol. 29, no. 5, p. 1807111, Feb. 2019, doi: <https://doi.org/10.1002/adfm.201807111>.
- [2] Z. Wang *et al.*, "Light-induced pyroelectric effect as an effective approach for ultrafast ultraviolet nanosensing," *Nat. Commun.*, vol. 6, no. 1, p. 8401, 2015, doi: [10.1038/ncomms9401](https://doi.org/10.1038/ncomms9401).
- [3] S. Sahare *et al.*, "Pyro-phototronic effect: An effective route toward self-powered photodetection," *Nano Energy*, vol. 107, Elsevier, p. 108172, Mar. 01, 2023, doi: [10.1016/j.nanoen.2023.108172](https://doi.org/10.1016/j.nanoen.2023.108172).
- [4] L. Zhu and Z. L. Wang, "Recent Progress in Piezo-Phototronic Effect Enhanced Solar Cells," *Adv. Funct. Mater.*, vol. 29, no. 41, p. 1808214, Oct. 2019, doi: [10.1002/ADFM.201808214](https://doi.org/10.1002/ADFM.201808214).
- [5] K. Maity *et al.*, "Piezo-phototronic effect in highly stable CsPbI₃-PVDF composite for self-powered nanogenerator and photodetector," *Nano Energy*, vol. 92, p. 106743, Feb. 2022, doi: [10.1016/J.NANOEN.2021.106743](https://doi.org/10.1016/J.NANOEN.2021.106743).
- [6] A. R. Jayakrishnan *et al.*, "Inorganic ferroelectric thin films and their composites for flexible electronic and energy device applications: current progress and perspectives," *Journal of Materials Chemistry C*, vol. 11, no. 3. The Royal Society of Chemistry, pp. 827–858, Jan. 19, 2022, doi: [10.1039/d2tc04424b](https://doi.org/10.1039/d2tc04424b).
- [7] J. P. B. Silva *et al.*, "Large ferro-pyro-phototronic effect in 0.5Ba(Zr 0.2 Ti 0.8)O 3-0.5(Ba 0.7 Ca 0.3)TiO 3 thin films integrated on silicon for photodetection," 2022, doi: [10.1002/cey2.297](https://doi.org/10.1002/cey2.297).
- [8] A. B. Swain, M. Rath, S. Pal, M. S. Ramachandra Rao, V. Subramanian, and P. Murugavel, "Self-polarization effect on large photovoltaic response in lead free ferroelectric 0.5Ba(Zr0.2Ti0.8)O3-0.5(Ba0.7Ca0.3)TiO3 epitaxial film," *Appl. Phys. Lett.*, vol. 113, no. 23, p. 233902, Dec. 2018, doi: [10.1063/1.5068699](https://doi.org/10.1063/1.5068699).
- [9] J. P. B. Silva *et al.*, "Ferroelectric phase transitions studies in 0.5Ba(Zr0.2Ti0.8)O3-0.5(Ba0.7Ca0.3)TiO3 ceramics," *J. Electroceramics*, vol. 35, no. 1–4, pp. 135–140, Dec. 2015, doi: [10.1007/S10832-015-0005-Y/METRICS](https://doi.org/10.1007/S10832-015-0005-Y/METRICS).
- [10] Y. Liu, Y. Ji, Y. Xia, L. Wu, C. R. Bowen, and Y. Yang, "Enhanced photocurrent in ferroelectric Bi0.5Na0.5TiO3 materials via ferro-pyro-phototronic effect," *Nano Energy*, vol. 98, p. 107312, Jul. 2022, doi: [10.1016/J.NANOEN.2022.107312](https://doi.org/10.1016/J.NANOEN.2022.107312).
- [11] K. Zhao, B. Ouyang, and Y. Yang, "Enhancing Photocurrent of Radially Polarized Ferroelectric BaTiO3 Materials by Ferro-Pyro-Phototronic Effect," *iScience*, vol. 3, pp. 208–216, May 2018, doi: [10.1016/J.ISCI.2018.04.016](https://doi.org/10.1016/J.ISCI.2018.04.016).
- [12] J. P. B. Silva *et al.*, "High-performance self-powered photodetectors achieved through the pyro-phototronic effect in Si/SnOx/ZnO heterojunctions," *Nano Energy*, vol. 89, no. May, p. 106347, Nov. 2021, doi: [10.1016/j.nanoen.2021.106347](https://doi.org/10.1016/j.nanoen.2021.106347).
- [13] J. P. B. Silva *et al.*, "Perovskite ferroelectric thin film as an efficient interface to enhance the photovoltaic characteristics of Si/SnOx heterojunctions," *J. Mater. Chem. A*, vol. 8, no. 22, pp. 11314–11326, 2020, doi: [10.1039/D0TA02198A](https://doi.org/10.1039/D0TA02198A).
- [14] J. P. B. Silva *et al.*, "High-Performance Ferroelectric–Dielectric Multilayered Thin Films for Energy Storage Capacitors," *Adv. Funct. Mater.*, vol. 29, no. 6, Feb. 2019, doi: [10.1002/adfm.201807196](https://doi.org/10.1002/adfm.201807196).
- [15] S. Qiao, H. Sun, J. Liu, G. Fu, and S. Wang, "The nanowire length dependence of the photoresponse and Pyro-phototronic response in the ZnO-based heterojunctions," *Nano Energy*, vol. 95, p. 107004, May 2022, doi: [10.1016/J.NANOEN.2022.107004](https://doi.org/10.1016/J.NANOEN.2022.107004).
- [16] M. Xue, W. Peng, X. Tang, Y. Cai, F. Li, and Y. He, "Pyro-Phototronic Effect Enhanced Pyramid Structured p-Si/n-ZnO Nanowires Heterojunction Photodetector," *ACS Appl. Mater. Interfaces*, vol. 15, p. 4689, Jan. 2022, doi: [10.1021/ACSAMI.2C18011/ASSET/IMAGES/LARGE/AM2C18011_0006.JPEG](https://doi.org/10.1021/ACSAMI.2C18011/ASSET/IMAGES/LARGE/AM2C18011_0006.JPEG).